

LONG TERM BEHAVIOUR OF A TYPE IIP SUPERNOVA SN 2004DJ IN THE RADIO BANDS

NAYANA A. J.,¹ POONAM CHANDRA,^{1,2} AND ALAK K. RAY³

¹*National Centre for Radio Astrophysics, Tata Institute of Fundamental Research, PO Box 3, Pune, 411007, India*

²*Department of Astronomy, Stockholm University, AlbaNova, SE-106 91 Stockholm, Sweden*

³*Homi Bhabha Centre for Science Education, Tata Institute of Fundamental Research, Mankhurd, Mumbai, 400088 India*

(Received June, 2018; Revised July, 2018; Accepted July 4, 2018)

Submitted to ApJ

ABSTRACT

We present radio observations and modelling of one of the nearest and brightest Type IIP supernova SN 2004dj exploded in the galaxy NGC 2403 at a distance of ~ 3.5 Mpc. Our observations span a wide frequency and temporal range of 0.24 - 43 GHz and ~ 1 day to 12 years since the discovery. We model the radio light curves and spectra with the synchrotron emission. We estimate the mass-loss rate of the progenitor star to be $\dot{M} \sim 1 \times 10^{-6} M_{\odot} \text{yr}^{-1}$ for a wind speed of 10 km s^{-1} . We calculate the radio spectral indices using 1.06, 1.40, 5.00 and 8.46 GHz flux density measurements at multiple epochs. We witness steepening in the spectral index values for an extended period predominantly at higher frequencies. We explain this as a signature of electron cooling happening at the supernova shock in the plateau phase of the supernova. We estimate the cooling timescales for inverse Compton cooling and synchrotron cooling and find that inverse Compton cooling is the dominant cooling process.

Keywords: Supernovae: general — supernovae: SN 2004dj — radiation mechanisms: non-thermal — circumstellar matter — radio continuum: general

arXiv:1808.00283v1 [astro-ph.HE] 1 Aug 2018

1. INTRODUCTION

Massive stars ($M > 8M_{\odot}$) end their lives in spectacular explosions called core-collapse supernovae (SNe). Type II SNe are explosions of massive stars that retain their hydrogen envelope at the time of explosions and show copious hydrogen emission lines in their optical spectra (Filippenko 1997). Type IIP SNe is a sub-class of Type II SNe characterized by a pronounced plateau of nearly constant luminosity in the optical light curve following a maximum that lasts for 80–120 days post explosion (Nadyozhin 2003). The plateau in their optical light curves is attributed to an extended hydrogen envelope intact to the star during explosion (Grasberg et al. 1971; Falk & Arnett 1977; Smartt 2009). In a volume limited sample (< 60 Mpc) of all core-collapse SNe, 48% is comprised by SNe IIP (Smith et al. 2011). Thus, SNe IIP is the most commonly observed variety of core-collapse SNe in the local universe and hence likely to be the most common evolutionary path in the end stages of the life of massive stars.

Several lines of evidence from stellar evolution models and supernova (SN) light curve models suggest that the progenitors of SNe IIP are red-supergiants (RSGs; Chevalier et al. 2006). The pre-supernova radius estimated from the plateau brightness and duration also falls in the typical RSG stellar radius ($10^{2-3}R_{\odot}$; Grasberg et al. 1971; Falk & Arnett 1977). RSGs are also identified as the progenitor stars of SNe IIP SNe in direct detection efforts (Smartt 2009). However, the masses of progenitor stars detected from pre-explosion images range from $8 - 15M_{\odot}$ (Van Dyk et al. 2003; Li et al. 2005, 2006; Maund & Smartt 2005; Maund et al. 2005) which is closer to the lower mass end for a core-collapse event. No RSG star of mass $M > 17M_{\odot}$ has been identified as a progenitor star of SNe IIP in direct detection efforts carried out in a volume limited sample (Smartt et al. 2009). In this context, a detailed census of type IIP SNe progenitors and the diversity of the properties of the SNe are important.

In a Type IIP SN, the fast moving stellar ejecta interacts with the circumstellar medium (CSM) created by the stellar wind of the progenitor star. The interaction creates a strong shock that moves ahead of the ejecta and is called the forward shock (Chevalier 1982). Electrons are accelerated to relativistic energies at the forward shock and emit at radio frequencies. Radio emission is absorbed at early times by either free-free absorption (FFA) or synchrotron self absorption (SSA) and can be modelled as synchrotron emission affected by either or both absorption processes. Depending on the dominant absorption process, various physical parameters like mass-loss rate of the progenitor star, density of the

CSM, ejecta density profile, shock deceleration parameter, magnetic field strength etc can be constrained from the modelled radio light curves and spectra (Chevalier 1982, 1998). On the other hand, X-ray emission from Type IIP SNe can be either thermal or non-thermal in origin. Thermal X-rays can be emitted from the hot forward and/or reverse shock regions whereas non-thermal X-ray emission can be due to the Inverse Compton (IC) scattering. In Type IIP SNe, the plateau of the optical light curve is a phase of high density of ambient photons which can be IC scattered to X-ray energies by the relativistic electrons. As a result of IC scattering the relativistic electrons lose energy and there is a corresponding cooling break in the radio spectra above a characteristic frequency (Chevalier et al. 2006).

In this work, we present long-term (~ 12 years) radio monitoring of a Type IIP, SN 2004dj over a frequency range of 0.24 to 43 GHz. We model the radio light curves and spectra with the standard mini-shell model (Chevalier 1982, 1998) and derive the mass-loss rate of the progenitor star. We also search for the signatures of cooling in the radio spectra and interpret our results in light of other published results.

The paper is organised as follows: In §2, we discuss the previous work published on SN 2004dj. In §3, we present the GMRT and VLA observations of SN 2004dj in detail. In §4, we describe the standard model for radio emission. In §5, we calculate the mass-loss rate of the progenitor star from the modelled parameters. In §6, we discuss the evolution of spectral indices and the signatures of cooling in the radio spectra. We summarise our main results in §7.

2. SN 2004DJ

SN 2004dj was discovered by K. Itagaki (Nakano et al. 2004) in NGC 2403 on 2004 July 31 (UT; all dates in this paper are in UT) with a visual magnitude of 11.2 mag at a position of $\alpha_{J2000} = 07^{\text{h}}37^{\text{m}}17.02^{\text{s}}$, $\delta_{J2000} = +65^{\circ}35'57.8''$. The SN was classified as a type IIP event from the optical spectrum taken on 2004 Aug 03.17 (Patat et al. 2004). SN 2004dj was discovered during the plateau phase i.e ~ 1 month after the explosion and hence the maxima of the optical light curve was not observed.

There is a large uncertainty in the explosion date of the SN. Zhang et al. (2006) derived an explosion date of 2004 June 10 \pm 21 assuming that SN 2004dj evolves like SN 1999em. Chugai et al. (2005) derived an explosion date of 2004 June 13 assuming that the light curves of SN 2004dj and SN 1999gi are similar. From the first one year of optical light curve of SN 2004dj, Vinkó et al. (2006) inferred an explosion date of 2004

June 30 ± 20 using Expanding Photosphere Method (EPM). Chugai et al. (2007) used an explosion date of 2004 June 28 to fit the H α lines (Korcakova et al. 2005) observed on day 55 and 64 post-explosion. We assume the date of explosion as 2004 June 28 through out this paper since this is the latest among the series of papers that report the explosion dates and is consistent with the majority of the other explosion dates reported in the literature within error bars.

Patat et al. (2004) reported the photospheric expansion velocities of H α , H β , Fe II (516.9 nm), Fe II (501.8 nm) and Fe II (492.4 nm) lines from the spectra obtained on 2004 Aug 3.17 as 6700, 5500, 4150, 3800 and 3850 km s $^{-1}$ respectively. Vinkó et al. (2006) reported the radial velocities of the SN ejecta from H α lines ranging from 6790 to 4256 km s $^{-1}$ on 33 to 99 days post-explosion, assuming the date of explosion as 2004 June 30 ± 20 . Chugai et al. (2007) derived the velocity from optical lines for SN 2004dj on day ~ 64 as 8200 km s $^{-1}$ assuming an explosion date of 2004 June 28.

The progenitor massive star of SN 2004dj is identified to be a member of the compact star cluster Sandage 96 (S96) from the archival data (Maíz-Apellániz 2004). For a cluster age of 13.6 Myr, Maíz-Apellániz et al. (2004) inferred the mass of progenitor star as $15 M_{\odot}$. Wang et al. (2005) derived a cluster age of ~ 20 Myr and the progenitor stellar mass as $\sim 12 M_{\odot}$. Vinkó et al. (2006) estimated the progenitor mass by fitting the spectral energy distribution of S96 with theoretical models. While the solutions were similar to that of Maíz-Apellániz et al. (2004) and Wang et al. (2005), an additional solution resulted in a cluster age ~ 8 Myr and progenitor mass of $M > 20 M_{\odot}$. It is interesting to note that, for any type IIP SNe, the highest progenitor mass detected from direct methods is $15 M_{\odot} < M_{\text{ZAMS}} < 20 M_{\odot}$ (for SN 1999ev; Maund & Smartt 2005).

SN 2004dj was observed in different wave bands of electromagnetic spectrum like infrared (IR; Kotak et al. 2005; Sugerman et al. 2005), X-ray (Pooley & Lewin 2004) and radio (Chandra & Ray 2004; Stockdale et al. 2004; Beswick et al. 2005). SN 2004dj exploded at a distance of $D \sim 3.1$ Mpc (Freedman et al. 2001) and is one of the nearest Type IIP event. Vinkó et al. (2006) inferred a distance of $D = 3.47 \pm 0.29$ Mpc to the host galaxy NGC 2403 from standard candle method and EPM. The distance to SN 2004dj is taken as $D = 3.47$ Mpc through out this paper.

2.1. Published radio and X-ray observations

Radio emission was detected from SN 2004dj at 8.4 GHz on 2004 Aug 02 with the Very Large Array (VLA; Stockdale et al. 2004). The first detection at 5 GHz was

made with the Multi-Element Radio Linked Interferometer Network (MERLIN) on 2004 Aug 5 with a flux density of 1.50 ± 0.15 mJy (Argo et al. 2004). Radio emission was also detected at 1.4 GHz with the Giant Metrewave Radio Telescope (GMRT; Chandra & Ray 2004). Beswick et al. (2005) monitored SN 2004dj with the MERLIN at 5 GHz starting from 2004 Aug 5 to Dec 2. At later epochs, the flux density of the SN was decreasing and hence the MERLIN observations placed a limit on the time of the peak of 5 GHz light curve (Beswick et al. 2005). Assuming the first detection at 5 GHz on 2004 Aug 5 to be coincident with the peak of light curve, Beswick et al. (2005) estimated the peak spectral luminosity as $L_{6 \text{ cm peak}} = 2.45 \times 10^{25}$ erg s $^{-1}$ Hz $^{-1}$. This peak spectral luminosity is comparable to that of SN 1999em i.e 2.2×10^{25} erg s $^{-1}$ Hz $^{-1}$ (Pooley et al. 2002).

X-ray emission was detected from SN 2004dj (Pooley & Lewin 2004) with the *Chandra X-ray observatory* on 2004 Aug 9. *Chandra* observations of SN 2004dj was carried out at four epochs (2004 Aug 9, Aug 23, Oct 3 and Dec 22) and Chakraborti et al. (2012) jointly fitted the X-ray spectra with the combination of a power law (IC component) and collisionally ionized diffuse gas (thermal component). From thermal X-ray emission, they measured the mass-loss rate of the progenitor star as $\dot{M} = (3.2 \pm 1.1) \times 10^{-7} M_{\odot} \text{yr}^{-1}$. From the combination of radio, optical and X-ray data, Chakraborti et al. (2012) derived the fraction of post shock energy density used in the amplification of magnetic fields to be $\epsilon_B = 0.082$ and in accelerating electrons to relativistic energies to be $\epsilon_e = 0.39$.

3. OBSERVATIONS AND DATA ANALYSIS

The VLA started observing SN 2004dj from 2004 Aug 02.9 UT. The observations were carried out in the 8.46, 22.46 and 43.34 GHz bands. Radio emission was detected from the SN in the 8.46 GHz band (Stockdale et al. 2004). Eventually, the SN was extensively observed in all VLA bands from 1.4 GHz (L-band) to 44 GHz band. J0642+679 and J0921+622 have been used as the phase calibrators to correct for the phase variations due to atmospheric fluctuations. 3C48 and 3C286 have been used as the primary calibrators to calibrate the flux density scale.

The GMRT started observing SN 2004dj from 2004 Aug 12 and detected radio emission from the SN at 1.4 GHz (Chandra & Ray 2004). Extensive follow-up observations were carried out with the GMRT at multiple epochs in the 1.4, 0.610, 0.325 and 0.235 GHz bands till 2016. 3C48 and 3C286 were used as the flux density cal-

ibrators, whereas J0835+555, J0614+607, J0614+617 and J0617+604 were used as the phase calibrator.

Both the VLA and GMRT data were analyzed using standard Astronomical Image Processing software (AIPS) packages. Few data sets were not used due to the bad quality. We also included the 5 GHz MERLIN observations from [Beswick et al. \(2005\)](#) for further analysis.

3.1. Radio lightcurves and spectral indices

We present the complete radio light curves at frequencies 0.24, 0.33, 0.61, 1.06, 1.4, 4.86, 1.994, 8.46, 14.94, 22.46 and 43.34 GHz in Figure 1. All the light curves except the 1.4 and 1.06 GHz light curves are in the optically thin phase of the evolution. We also present the radio spectral index α ($F_\nu \propto \nu^\alpha$) using the flux density measurements at 1.06, 1.40, 5 and 8.46 GHz at various epochs in Figure 2. The temporal evolution of the spectral indices between 1.39 and 4.99 GHz traces the transition from optically thick to thin phase of the SN. The spectral indices between 4.86 and 8.46 GHz show values as steep as -1 and even lower for an extended period of time from \sim day 50 to 150 post explosion. These values are steeper than the expected optically thin spectral indices of Type II SNe. We explain this trend in detail in terms of cooling in a later section (see §6.2).

4. A RADIO MODEL

We fit the data with the standard mini-shell model in which radio emission is purely synchrotron with either synchrotron self absorption (SSA) or free-free absorption (FFA) as the dominant absorption process ([Chevalier 1982, 1998](#)). The model assumes that the magnetic field energy density and the energy density of relativistic electrons are proportional to the post shock energy density (model 1 of [Chevalier 1996](#)). The temporal and spectral evolution of radio flux density and optical depth can be modelled. The FFA model was proposed by [Chevalier \(1982\)](#) and was developed in detail by [Van Dyk et al. \(1994\)](#) and [Weiler et al. \(2002\)](#) later. The radio flux density, $S(\nu, t)$, with FFA as the dominant absorption can be written as:

$$S(\nu, t) = K_1 \left(\frac{\nu}{5 \text{ GHz}} \right)^\alpha \left(\frac{t}{100 \text{ day}} \right)^\beta e^{-\tau_{\text{ffa}}} \quad (1)$$

$$\tau_{\text{ffa}} = K_2 \left(\frac{\nu}{5 \text{ GHz}} \right)^{-2.1} \left(\frac{t}{100 \text{ day}} \right)^\delta \quad (2)$$

where α is the optically thin spectral index ($F_\nu \propto \nu^\alpha$), which is related to the electron energy index p ($N(E) \propto E^{-p}$) as $\alpha = -(p-1)/2$. Here K_1 and K_2 are the flux density and optical depth normalizations, respectively.

' t ' denotes the days since explosion assuming a date of explosion 2004 June 28 ([Chugai et al. 2007](#)). The parameter δ is related to the shock deceleration parameter m ($R \propto t^m$) as $\delta = -3m$. The parameter δ is essentially constrained by the evolution of the optical depth in time. If we look at the light curves (see Figure 1) there are not enough simultaneous multi-frequency measurements in the optically thick part to allow the derivation of the optical depth behaviour in time. [Weiler et al. \(1986\)](#) and [Chevalier \(1984\)](#) suggest that in these cases it is recommended to do the fit with 4 parameters where $\delta = (-3 + \alpha - \beta)$. We fit the full data with the FFA model keeping K_1 , K_2 , α and β as the free parameters.

We use the formulation of SSA model from ([Chevalier 1998](#)). The variation of radio flux density and SSA optical depth can be written as:

$$S(\nu, t) = K_1 \left(\frac{\nu}{5 \text{ GHz}} \right)^{5/2} \left(\frac{t}{100 \text{ day}} \right)^a (1 - e^{-\tau_{\text{ssa}}}) \quad (3)$$

$$\tau_{\text{ssa}} = K_2 \left(\frac{\nu}{5 \text{ GHz}} \right)^{-(p+4)/2} \left(\frac{t}{100 \text{ day}} \right)^{-(a+b)} \quad (4)$$

Here, a and b denote the temporal index of the radio flux density in the optically thick ($F \propto t^a$) and thin phases ($F \propto t^{-b}$), respectively. Assuming the energy density in the magnetic field and relativistic electrons are proportional to the post-shock energy density (model 1 of [Chevalier 1996](#)), the shock deceleration parameter m is related to a , b and p as $a = 2m + 0.5$ in the optically thick phase and $b = (p + 5 - 6m)/2$ in the optically thin phase ([Chevalier 1998](#)).

We perform a two variable (ν, t) fit to the complete data for both FFA and SSA models. The free parameters are K_1 , K_2 , α and β in the FFA model and K_1 , K_2 , m and p in the SSA model. FFA and SSA model fits with the data with reduced chi-square values of 1.78 and 1.51 respectively. The best-fit parameters for both FFA and SSA model fits are given in Table 2. Figure 3 and 4 shows the model fits along with the observed flux density measurements. While the reduced chi-square value for SSA model is marginally better than that of FFA model, it is difficult to infer that either of the models fit the data better from visual inspection or from the reduced chi-square values. This is due to the sparse data available in the optically thick regime. We derive the shock deceleration parameter $m = 0.93 \pm 0.02$ and $m = 0.97 \pm 0.01$ for FFA and SSA models respectively.

We also repeated the modelling with the date of explosion as 2004 June 10 ([Zhang et al. 2006](#)). The reduced chi-square and physical parameters are not significantly

Table 1. Details of radio observations of SN 2004dj

Date of Observation (UT)	Age ^a (day)	Frequency (GHz)	Supernova		Phase Calibrator		Telescope
			F_ν (mJy)	rms (mJy beam ⁻¹)	Name	F_ν (Jy)	
2004 Aug 1.88	34.12	8.46	1.28 ± 0.046	0.046	J0642+679	0.32	VLA-D Array
2004 Aug 1.90	34.14	22.46	< 0.429	0.169	J0642+679	0.15	VLA-D Array
2004 Aug 2.88	35.12	8.46	1.6 ± 0.090	0.09	J0921+622	0.78	VLA-D Array
2004 Aug 2.89	35.13	22.46	<1.095	0.416	J0921+622	0.67	VLA-D Array
2004 Aug 2.91	35.15	43.32	<0.956	0.478	J0921+622	0.55	VLA-D Array
2004 Aug 5.00	37.24	8.46	1.780 ± 0.289	0.228	J0921+622	0.78	VLA-D Array
2004 Aug 5.01	37.25	22.46	<1.593	0.531	J0921+622	0.61	VLA-D Array
2004 Aug 5.02	37.26	4.86	2.070 ± 0.322	0.247	J0921+622	0.8	VLA-D Array
2004 Aug 5.08	37.32	14.94	<0.870	0.290	J0921+622	0.54	VLA-D Array
2004 Aug 5.5	37.74	4.99	1.8 ± 0.3^b	0.3	–	–	MERLIN
2004 Aug 8.8	41.04	4.99	1.8 ± 0.3^b	0.3	–	–	MERLIN
2004 Aug 9.82	42.06	8.46	1.217 ± 0.188	0.143	J0921+622	0.78	VLA-D Array
2004 Aug 9.83	42.07	4.86	2.133 ± 0.277	0.177	J0921+622	0.8	VLA-D Array
2004 Aug 11.40	43.64	4.99	2.1 ± 0.3^b	0.3	–	–	MERLIN
2004 Aug 12.24	44.24	1.39	0.39 ± 0.17	0.07	J0614+607	0.97	GMRT
2004 Aug 13.78	46.02	14.94	0.799 ± 0.206	0.19	J0921+622	0.61	VLA-D Array
2004 Aug 13.80	46.04	4.86	2.258 ± 0.299	0.196	J0921+622	0.80	VLA-D Array
2004 Aug 13.80	46.04	8.46	1.349 ± 0.192	0.137	J0921+622	0.78	VLA-D Array
2004 Aug 13.82	46.06	22.46	<1.551	0.517	J0921+622	0.54	VLA-D Array
2004 Aug 14.50	46.74	4.99	1.88 ± 0.3^b	0.3	–	–	MERLIN
2004 Aug 20.66	52.90	8.46	<1.8	0.644	J0921+622	0.78	VLA-D Array
2004 Aug 20.67	52.91	4.86	1.72 ± 0.089	0.089	J0921+622	0.8	VLA-D Array
2004 Aug 22.00	54.24	1.39	0.67 ± 0.23	0.10	J0617+604	1.4	GMRT
2004 Aug 22.00	54.24	1.06	< 0.26	0.13	J0614+617	1.19	GMRT
2004 Aug 23.40	55.64	4.994	1.75 ± 0.3^b	0.3	–	–	MERLIN
2004 Aug 26.54	58.78	8.46	0.839 ± 0.262	0.065	J0921+622	0.80	VLA-D Array
2004 Aug 26.55	58.78	4.86	1.282 ± 0.083	0.083	J0921+622	0.81	VLA-D Array
2004 Aug 26.60	58.84	4.99	1.125 ± 0.3^b	0.3	–	–	MERLIN
2004 Aug 29.60	61.84	4.99	1.25 ± 0.3	0.3	–	–	MERLIN
2004 Aug 29.65	61.88	14.94	<0.5	0.158	J0921+622	0.74	VLA-D Array
2004 Aug 29.66	61.89	4.86	1.26 ± 0.088	0.088	J0921+622	0.8	VLA-D Array
2004 Aug 29.67	61.90	8.46	0.83 ± 0.079	0.079	J0921+622	0.78	VLA-D Array
2004 Aug 29.68	61.91	22.46	<0.450	0.149	J0921+622	0.77	VLA-D Array
2004 Sep 01.00	64.24	1.39	0.72 ± 0.22	0.075	J0614+607	1.23	GMRT
2004 Sep 01.00	64.24	1.06	0.41 ± 0.12	0.12	J0614+607	1.42	GMRT

^aThe age is calculated assuming date of explosion as 2004 June 28.00 (UT)^bBeswick et al. (2005) and personal communication with Megan Argo.

Table 1. Details of radio observations of SN 2004dj (*continuation*)

Date of Observation (UT)	Age ^a (day)	Frequency (GHz)	Supernova		Phase Calibrator		Telescope
			F_ν (mJy)	rms (mJy beam ⁻¹)	Name	F_ν (Jy)	
2004 Sep 2.60	65.84	4.99	0.78 ± 0.3^b	0.3	–	–	MERLIN
2004 Sep 4.90	68.14	4.99	0.94 ± 0.3^b	0.3	–	–	MERLIN
2004 Sep 08.6	71.84	4.99	0.96 ± 0.3^b	0.3	–	–	MERLIN
2004 Sep 10.40	73.64	1.46	1.164 ± 0.180	0.138	J0921+622	0.9	VLA-A Array
2004 Sep 10.50	73.74	4.88	1.184 ± 0.086	0.062	J0921+622	0.76	VLA-A Array
2004 Sep 10.50	73.74	8.44	0.644 ± 0.062	0.05	J0921+622	0.75	VLA-A Array
2004 Sep 10.56	73.80	14.94	<0.753	0.251	J0921+622	0.74	VLA-A Array
2004 Sep 11.30	74.54	4.99	1.15 ± 0.3^b	0.3	–	–	MERLIN
2004 Sep 14.70	77.94	4.99	0.8 ± 0.3^b	0.3	–	–	MERLIN
2004 Sep 17.30	80.54	4.99	1.08 ± 0.3^b	0.3	–	–	MERLIN
2004 Sep 19.90	83.14	4.99	1.02 ± 0.3	0.3	–	–	MERLIN
2004 Sep 20.72	83.96	14.94	<0.835	0.3	J0921+622	0.73	VLA-A Array
2004 Sep 20.73	83.97	4.86	0.838 ± 0.137	0.069	J0921+622	0.73	VLA-A Array
2004 Sep 20.74	83.98	8.46	0.302 ± 0.073	0.051	J0921+622	0.72	VLA-A Array
2004 Sep 20.75	83.99	1.425	1.555 ± 0.158	0.087	J0921+622	0.88	VLA-A Array
2004 Sep 26.83	90.07	14.94	<0.708	0.236	J0921+622	0.74	VLA-A Array
2004 Sep 26.84	90.08	4.86	0.824 ± 0.128	0.07	J0921+622	0.73	VLA-A Array
2004 Sep 26.85	90.09	8.46	0.374 ± 0.095	0.059	J0921+622	0.72	VLA-A Array
2004 Sep 26.86	90.10	1.425	1.285 ± 0.187	0.098	J0921+622	0.85	VLA-A Array
2004 Sep 29.40	92.64	4.99	1.11 ± 0.3	0.3	–	–	MERLIN
2004 Sep 30.00	93.24	1.39	1.78 ± 0.58	0.23	J0614+607	1.93	GMRT
2004 Oct 02.00	95.24	4.99	0.88 ± 0.3^b	0.3	–	–	MERLIN
2004 Oct 03.70	96.94	4.994	0.90 ± 0.3^b	0.3	–	–	MERLIN
2004 Oct 5.60	98.84	1.425	1.498 ± 0.169	0.078	J0921+622	0.90	VLA-A Array
2004 Oct 5.61	98.85	4.86	1.091 ± 0.104	0.089	J0921+622	0.91	VLA-A Array
2004 Oct 5.62	98.86	8.46	0.524 ± 0.076	0.072	J0921+622	0.8	VLA-A Array
2004 Oct 5.63	98.87	22.46	<0.429	0.143	J0921+622	0.7	VLA-A Array
2004 Nov 16.50	140.74	4.99	0.820 ± 0.4^b	0.4	–	–	MERLIN
2004 Nov 23.50	147.74	4.99	0.68 ± 0.2	0.2	–	–	MERLIN
2004 Nov 23.52	147.76	1.425	1.402 ± 0.182	0.075	J0921+622	0.86	VLA-A Array
2004 Nov 23.54	147.78	4.86	0.649 ± 0.125	0.104	J0921+622	0.69	VLA-A Array
2004 Nov 23.55	147.79	8.46	0.401 ± 0.11	0.109	J0921+622	0.6	VLA-A Array
2004 Nov 23.55	147.79	22.46	<0.918	0.306	J0921+622	0.31	VLA-A Array
2004 Nov 26.50	150.74	4.99	0.39 ± 0.2^b	0.2	–	–	MERLIN
2004 Nov 30.51	154.75	22.46	0.282 ± 0.094	0.094	J0921+622	0.72	VLA-A Array

^aThe age is calculated assuming date of explosion as 2004 June 28.00 (UT).^bBeswick et al. (2005) and personal communication with Megan Argo.

Table 1. Details of radio observations of SN 2004dj (*continuation*)

Date of Observation (UT)	Age ^a (day)	Frequency (GHz)	Supernova		Phase Calibrator		Telescope
			F_ν (mJy)	rms (mJy beam ⁻¹)	Name	F_ν (Jy)	
2004 Nov 30.51	154.75	1.425	1.24 ± 0.154	0.091	J0921+622	0.87	VLA-A Array
2004 Nov 30.52	154.76	4.86	0.435 ± 0.059	0.055	J0921+622	0.77	VLA-A Array
2004 Nov 30.53	154.77	8.46	0.278 ± 0.045	0.043	J0921+622	0.79	VLA-A Array
2004 Dec 09.00	163.24	1.39	1.44 ± 0.18	0.07	J0617+604	1.25	GMRT
2004 Dec 10.00	164.24	1.06	1.74 ± 0.35	0.15	J0614+607	0.3	GMRT
2004 Dec 30.21	184.45	1.425	0.979 ± 0.132	0.081	J0921+622	0.86	VLA-A Array
2004 Dec 30.23	184.47	4.86	0.255 ± 0.084	0.07	J0921+622	0.75	VLA-A Array
2004 Dec 30.24	184.48	8.46	<0.180	0.059	J0921+622	0.80	VLA-A Array
2004 Dec 30.25	184.49	22.46	<0.567	0.189	J0921+622	0.65	VLA-A Array
2005 Jan 01.00	186.24	1.39	1.10 ± 0.14	0.05	J0617+604	1.21	GMRT
2005 Jan 01.00	187.24	1.06	1.62 ± 0.20	0.14	J0614+607	1.30	GMRT
2005 Jan 16.23	201.47	1.425	1.16 ± 0.281	0.164	J0921+622	0.88	VLA-BnA Array
2005 Jan 16.24	201.48	4.86	0.461 ± 0.09	0.07	J0921+622	0.81	VLA-BnA Array
2005 Jan 16.25	201.49	8.46	<0.129	0.045	J0921+622	0.88	VLA-BnA Array
2005 Feb 8.19	225.43	1.425	1.2 ± 0.295	0.125	J0921+622	0.86	VLA-BnA Array
2005 Feb 8.20	225.44	4.86	0.339 ± 0.079	0.065	J0921+622	0.78	VLA-BnA Array
2005 Feb 8.21	225.45	8.46	0.255 ± 0.063	0.044	J0921+622	0.87	VLA-BnA Array
2005-Feb-18.00	235.24	0.61	1.92 ± 0.28	0.17	J0834+555	8.16	GMRT
2005 Mar 15.00	260.24	1.39	0.92 ± 0.2	0.07	J0614+607	1.21	GMRT
2005 Mar 26.96	272.20	1.425	0.93 ± 0.2	0.125	J0921+622	0.94	VLA-B Array
2005 Mar 26.97	272.21	4.86	<0.341	0.07	J0921+622	0.89	VLA-B Array
2005 Mar 26.98	272.22	8.46	0.16 ± 0.058	0.036	J0921+622	0.84	VLA-B Array
2005 Apr 01.00	277.24	0.61	1.79 ± 0.16	0.243	J0834+555	8.755	GMRT
2005 Jun 12.81	349.05	1.425	<1.750	0.487	J0921+622	0.83	VLA-CnB Array
2005 Jun 12.82	349.06	4.86	0.317 ± 0.07	0.07	J0921+622	0.81	VLA-C Array
2005 Jun 12.84	349.08	8.44	<0.149	0.050	J0921+622	0.98	VLA-C Array
2005 Jun 13.78	350.02	22.485	<0.314	0.105	J0921+622	0.79	VLA-CnB Array
2005 Jun 13.79	350.03	8.44	0.184 ± 0.048	0.047	J0921+622	0.97	VLA-C Array
2005 Jun 13.82	350.06	14.94	<0.489	0.163	J0921+622	0.97	VLA-CnB Array
2005 Jun 13.82	350.06	1.425	<0.896	0.30	J0921+622	0.81	VLA-CnB Array
2005 Jun 13.84	350.08	4.885	0.322 ± 0.058	0.056	J0921+622	0.83	VLA-CnB Array
2005 Sep 11.91	440.15	8.46	<0.111	0.037	J0921+622	1.01	VLA-CnB Array
2006 Sep 25.54	818.78	1.425	0.507 ± 0.162	0.162	J0921+622	0.76	VLA-CnB Array
2006 Sep 25.55	818.79	4.86	<0.192	0.063	J0921+622	1.1	VLA-CnB Array

^aThe age is calculated using assuming date of explosion as 2004 June 28.00 (UT).

Table 1. Details of radio observations of SN 2004dj (*continuation*)

Date of Observation (UT)	Age ^a (day)	Frequency (GHz)	Supernova		Phase Calibrator		Telescope
			F_ν (mJy)	rms (mJy beam ⁻¹)	Name	F_ν (Jy)	
2007 May 15.24	1050.48	0.244	<10.47	3.949	J0834+555	8.70	GMRT
2007 May 18.41	1053.65	1.39	<0.510	0.169	J0834+555	9.54	GMRT
2007 May 22.37	1057.61	0.325	<3.549	1.183	J0834+555	9.77	GMRT
2007 May 28.84	1064.08	1.425	0.375 ± 0.102	0.058	J0921+622	0.81	VLA-A Array
2008 Oct 24.48	1578.72	1.425	0.228 ± 0.077	0.07	J0921+622	1.07	VLA-A Array
2008 Oct 24.50	1578.74	4.86	<0.109	0.046	J0921+622	1.50	VLA-A Array
2016 Nov 02.04	4187.28	1.39	<0.105	0.035	J0614+607	–	GMRT
2016 Oct 25.92	4180.16	0.610	<0.210	0.050	J0834+555	–	GMRT
2016 Nov 05.04	4190.28	0.325	<0.615	0.095	J0834+555	–	GMRT

^aThe age is calculated assuming date of explosion as 2004 June 28.00 (UT).

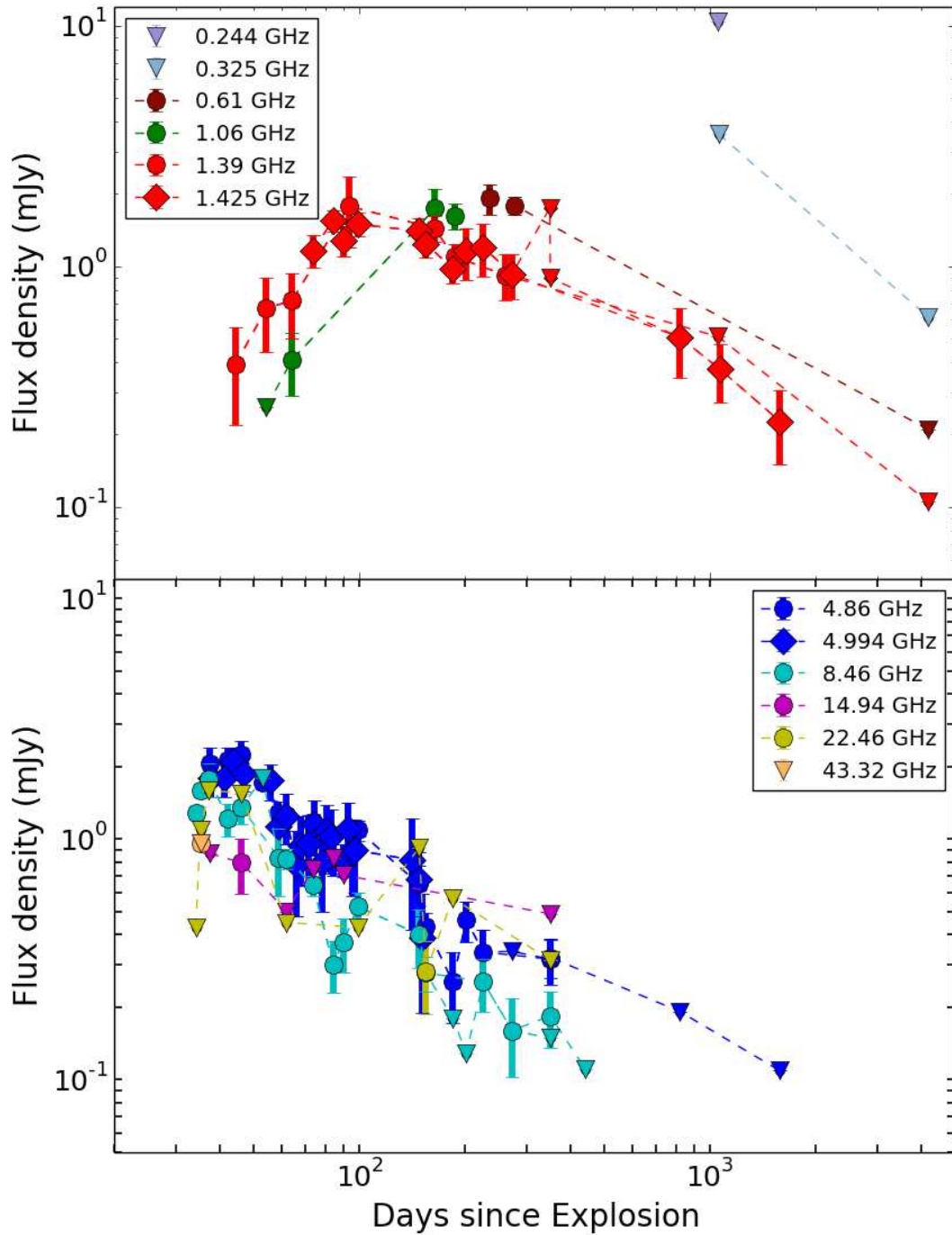


Figure 1. Upper panel: Light curves of SN 2004dj at frequencies 0.24, 0.33, 0.61, 1.06, 1.39 and 1.43 GHz. The 1.40 GHz data denoted in red color include both 1.39 GHz GMRT measurements (circles) and 1.43 GHz VLA measurements (diamonds). Lower panel: Light curves of SN 2004dj at frequencies 4.86, 4.99, 8.46, 14.94, 15.00, 22.46 and 43.32 GHz. Inverted triangles in both top and bottom panels denote 3σ upper limits. The days since explosion are calculated assuming the date of explosion as 2004 June 28 (UT).

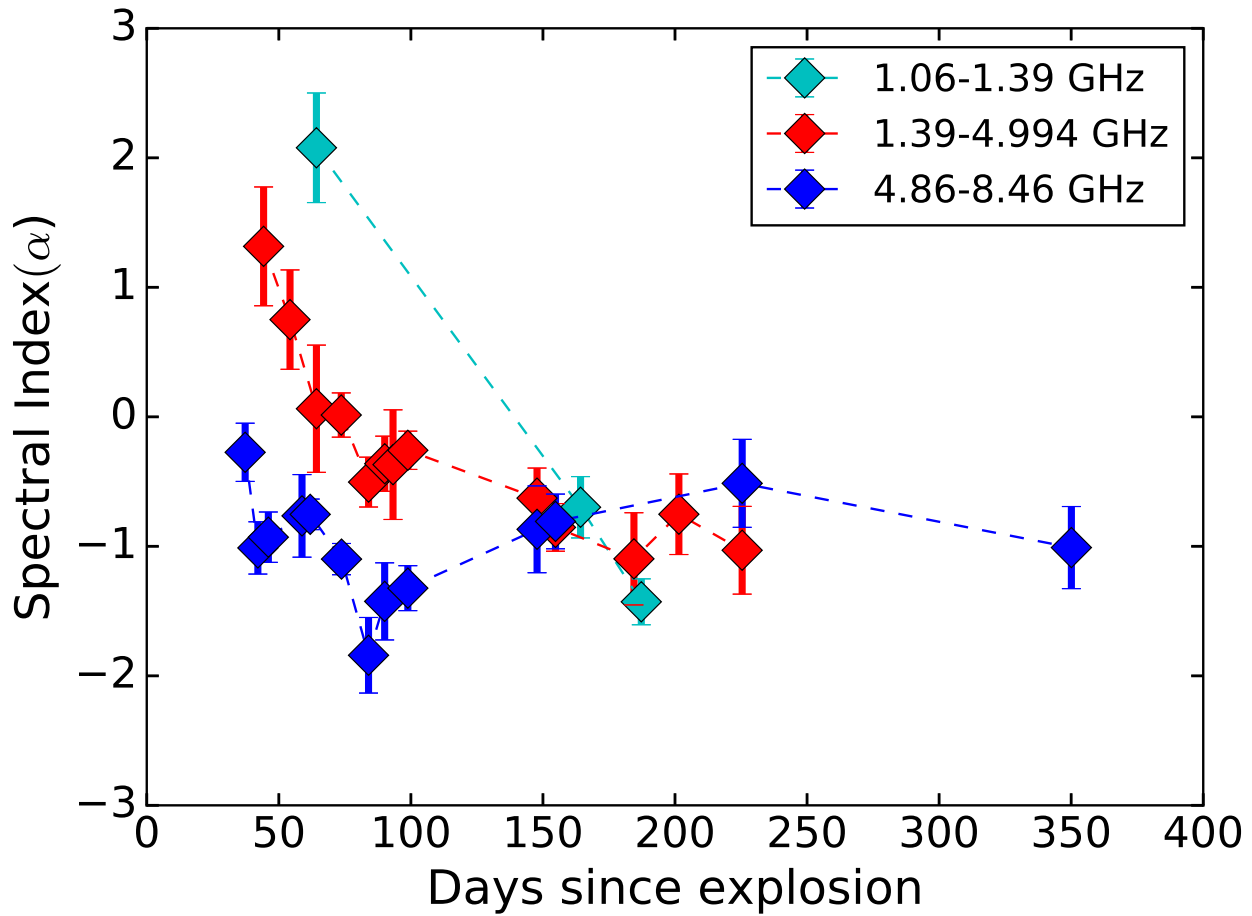


Figure 2. The radio spectral index variation for SN 2004dj. The figure shows the spectral index between frequencies 1.06/1.4, 1.4/4.9, 4.9/8.46 GHz. The days since explosion are calculated assuming the date of explosion as 2004 June 28 (UT). The spectral index curve between 4.9 GHz and 8.46 GHz shows a distinct dip around 75 days.

different from the previous values. While the date of explosion of SN 2004dj is uncertain due to the late discovery, our results are not critically sensitive to the exact date of explosion.

4.1. Dominant absorption mechanism

Since the FFA or SSA models cannot be clearly distinguished from the fits, we can look for other signatures that can disentangle the dominant absorption processes. Assuming SSA as the dominant absorption process that defines the peak flux density of the radio light curves, we can derive the size of the radio-emitting shell using the equation (Chevalier 1998):

$$R_p = 8.8 \times 10^{15} f_{eB}^{-1/19} \left(\frac{f}{0.5}\right)^{-1/19} \left(\frac{F_p}{\text{Jy}}\right)^{9/19} \times \left(\frac{D}{\text{Mpc}}\right)^{18/19} \left(\frac{\nu}{5 \text{ GHz}}\right)^{-1} \text{ cm} \quad (5)$$

Here f_{eB} is the equipartition factor defined as $f_{eB} = \epsilon_e/\epsilon_B$ where ϵ_e denotes the relativistic electron energy density and ϵ_B denotes the magnetic field energy density. F_p is the peak flux density of the light curve at frequency ν . f is the volume filling factor of the spherical emission region of radius R . D is the distance to the SN in units of Mpc. The equation for R_p is specifically for electron energy index $p = 3$ (Chevalier 1998). However, we use this formula since our best fit p value for SSA model is $p = 2.9$ which is very close to 3. The mean shell velocity $v_p = R_p/t$ where t is the time at which the light curve peaks. If the observed mean shell velocity is larger than this value, it means that SSA flux is low and other mechanism like FFA could be dominant in determining the peak flux. For SN 2004dj, the peak flux density at 5 GHz is $F_p = 1.8$ mJy on 2004 Aug 5 ($t_p = 38$ days; Beswick et al. 2005). We use $f_{eB} = 4.8$ (Chakraborti et al. 2012) and $f = 0.5$ (Chevalier 1998) to estimate the mean shell velocity $v_p \sim 4007 \text{ km s}^{-1}$ on ~ 38 days post explosion. The actual mean velocity obtained from optical line measurements can be now compared to this value. The velocity derived from the H_α lines for SN 2004dj on day ~ 36 (2004 Aug 3.17) is 6700 km s^{-1} (Patat et al. 2004) and is larger than the velocity deduced above. Vinkó et al. (2006) reports the radial velocities of the SN ejecta from H_α lines as 6790 on 2004 Aug 3. Chugai et al. (2007) reports the shell velocity to be $\sim 8200 \text{ km s}^{-1}$ on 64 days post explosion from H_α lines. Thus these observations are suggestive of FFA as the dominant absorption process. Chevalier et al. (2006) also suggest FFA as the dominant absorption process for SN 2004dj from the steep rise of 1.4 GHz light curve (Chandra & Ray 2004). We repeat

Table 2. Best fit parameters for FFA and SSA models

FFA	SSA
$K_1 = 0.82 \pm 0.02$	$K_1 = 62.46 \pm 07.01$
$K_2 = (3.01 \pm 0.35) \times 10^{-2}$	$K_2 = (1.27 \pm 0.15) \times 10^{-2}$
$\alpha = -0.92 \pm 0.05$	$m = 0.97 \pm 0.01$
$\beta = -1.13 \pm 0.06$	$p = 2.87 \pm 0.10$
$\chi_\mu^2 = 1.78$	$\chi_\mu^2 = 1.51$

NOTE— K_1 and K_2 are the normalization parameters of flux density and optical depth, respectively. In FFA model, α and β denotes the spectral and temporal evolution of the radio flux density. In the SSA model m denotes the shock deceleration parameter and p denotes the electron energy index.

this exercise using the 1.4 GHz light curve that peaks around day 93. The peak flux density is $F_p = 1.78$ mJy at 1.4 GHz and the deduced mean velocity is $v_p \sim 5830 \text{ km s}^{-1}$. The observed H_α line velocity on day 96 post explosion is 4373 km s^{-1} (Vinkó et al. 2006). However, Chugai et al. (2007) reports the observed shell velocity on day 98 post explosion to be $\sim 8000 \text{ km s}^{-1}$ from a prominent notch like feature in the spectra. This is also greater than the derived mean shell velocity and is indicative of FFA as the plausible absorption process.

5. MASS-LOSS RATE

Assuming FFA as the dominant absorption process, we derive the mass-loss rate of the progenitor star of SN 2004dj. The various assumptions that go into the calculation are as follows and are detailed in Weiler et al. (1986). The progenitor expels the outer layer of stellar material via constant stellar wind creating a density field around the star such that $\rho_{\text{wind}} \sim r^{-2}$. The wind material is completely ionized possibly due to the initial flash of radiation from the SN. Assuming electron ion equilibrium and the wind material to be singly ionized with cosmic abundance, the mass loss rate is given by Weiler et al. (1986) as

$$\dot{M} = 3.02 \times 10^{-6} \tau_{5 \text{ GHz}}^{0.5} \left(\frac{w}{10 \text{ km s}^{-1}}\right) \left(\frac{v_i}{10^4 \text{ km s}^{-1}}\right)^{1.5} \times \left(\frac{t_i}{45 \text{ days}}\right)^{1.5} \left(\frac{t}{t_i}\right)^{1.5m} m^{-1.5} \times \left(\frac{T_e}{10^4 \text{ K}}\right)^{0.68} M_\odot \text{ yr}^{-1} \quad (6)$$

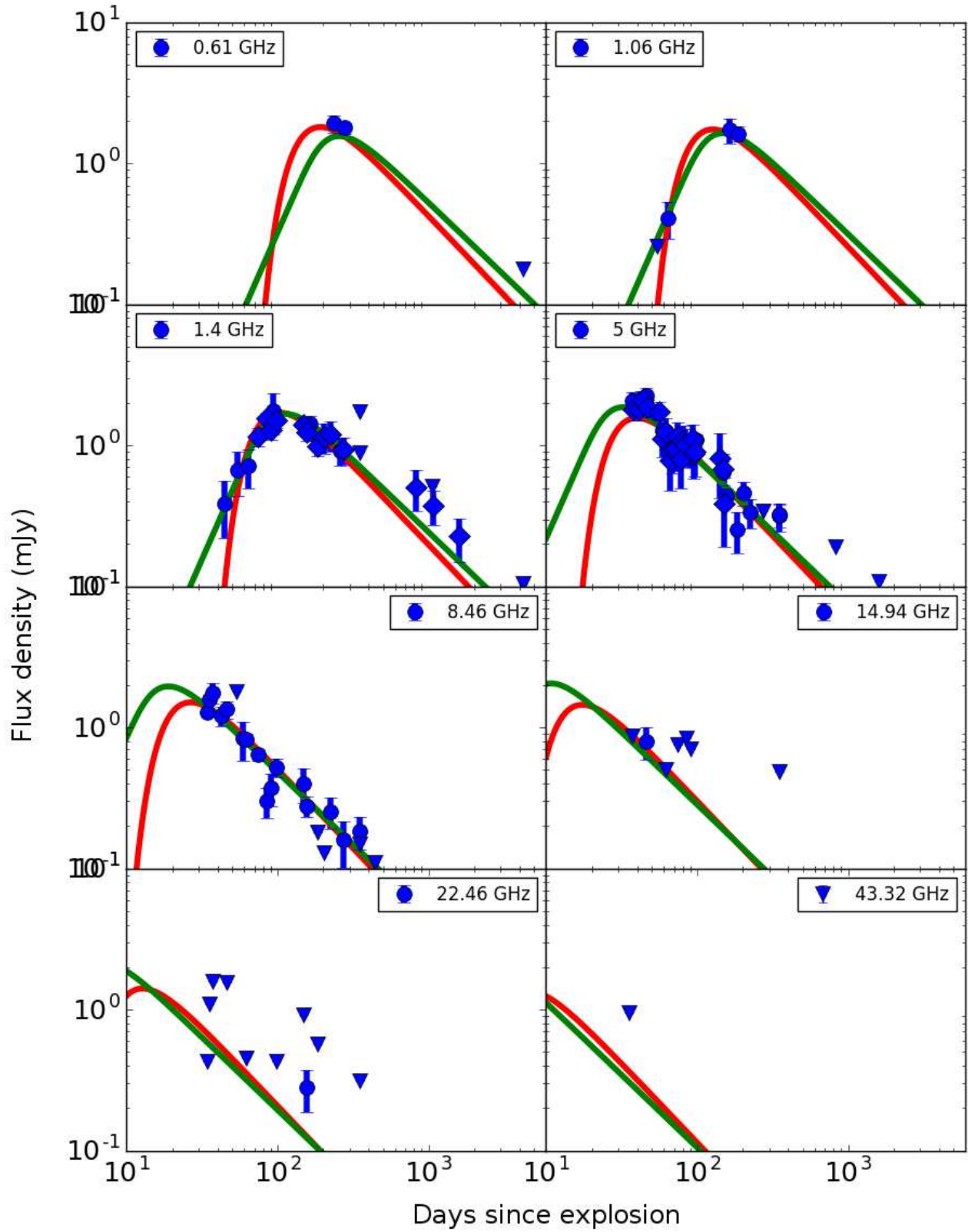


Figure 3. SSA and FFA model fit to the radio light curves of SN 2004dj at 0.61, 1.06, 1.4, 5.00, 8.46, 14.94, 22.46 and 43.34 GHz bands. The 1.40 GHz data includes both 1.39 GHz GMRT measurements (circles) and 1.43 GHz VLA measurements (diamonds). Green solid line denotes the SSA model and red solid line denotes the FFA model. The days since explosion is calculated assuming the date of explosion as 2004 June 28 (UT).

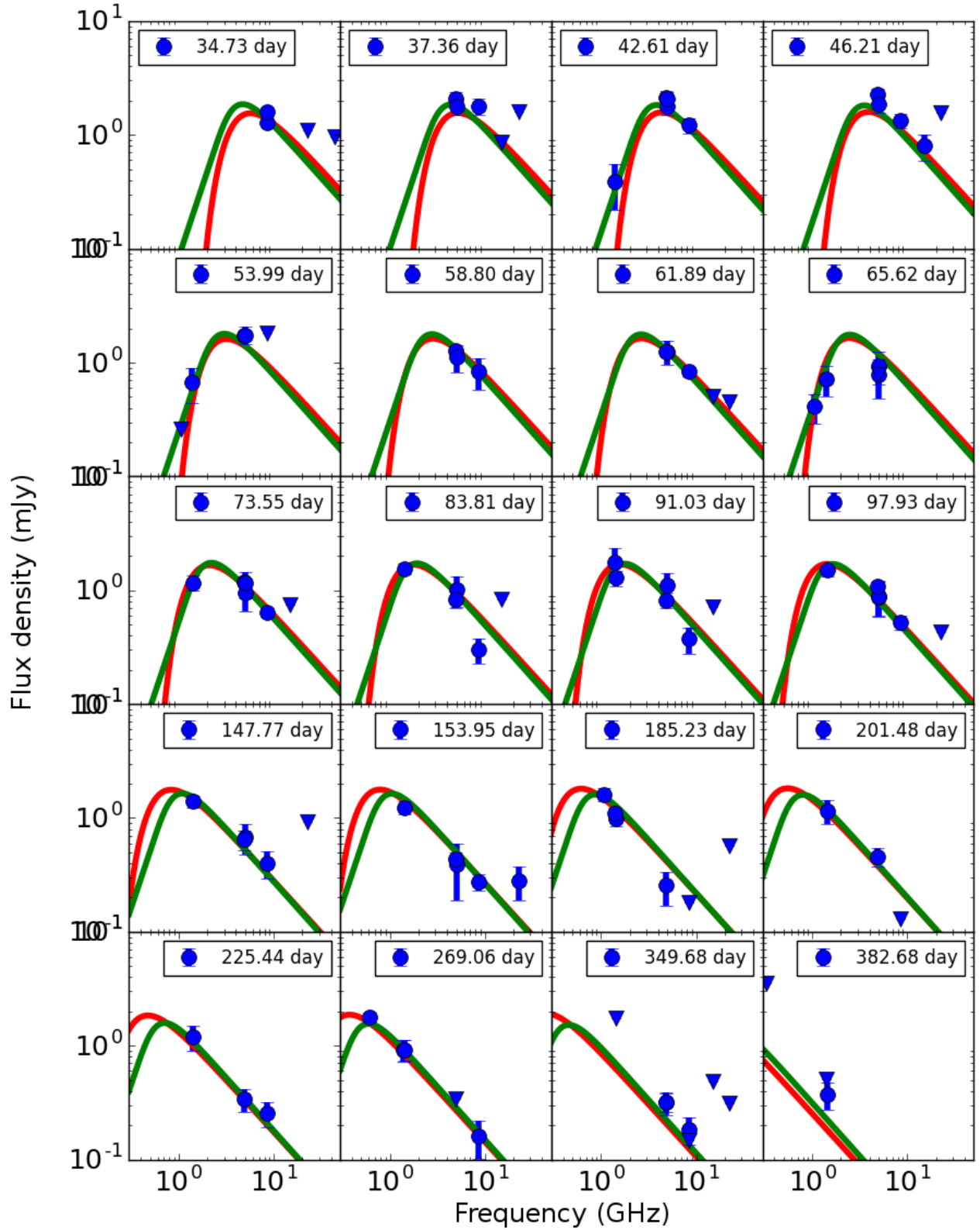


Figure 4. SSA and FFA model fit to the radio spectra of SN 2004dj on \sim day 35 to 383 post explosion. Green solid line denotes the SSA model and red solid line denotes the FFA model. The days since explosion is calculated assuming the date of explosion as 2004 June 28 (UT).

where w is the velocity of the stellar wind in km s^{-1} , v_i is the SN ejecta velocity in km s^{-1} at time t_i (days post explosion) inferred from optical line observations. T_e is the electron temperature in the stellar wind and is an uncertain parameter. We use $v_i = 8200 \text{ km s}^{-1}$, the highest velocity $H\alpha$ absorption feature seen in the optical spectra on $t_i = 64$ days (Chugai et al. 2007). From the modelled radio light curve (equation 2), we have $\tau_{5 \text{ GHz}}(\text{day } 100) = 0.03$ and $m = 0.93$. We derive the mass-loss rate of the progenitor star to be $\dot{M}/w1 = (1.37 \pm 0.11) T_{cs4}^{0.68} \times 10^{-6} M_{\odot} \text{yr}^{-1}$. Here $w1$ denotes the stellar wind velocity in units of 10 km s^{-1} and T_{cs4} denotes the CSM electron temperature in units of 10^4 K.

6. DISCUSSION

6.1. Progenitor properties

We model the radio observations with the standard mini-shell model (Chevalier 1982) as explained in §4. We estimate the shock deceleration parameter $m \sim 0.9$ (where $R \propto t^m$) for FFA model indicative of a mildly decelerating blast wave. This is in accord with the physics of the process as the blast wave is interacting with the CSM and is expected to slow down. The range of m values for Type II SNe is $m = 0.8 - 1$ (Weiler et al. 1986). For a shocked shell of radius $R \sim t^{0.9}$, the ejecta density index n ($\rho \sim r^{-n}$) is given by $m = (n-3)/(n-2)$, assuming that the CSM is created by a steady stellar wind of density ($\rho \sim r^{-2}$) (Chevalier 1982). Thus for $m \sim 0.9$, we derive the power law ejecta density as $\rho \sim r^{-11.4}$. The progenitors of Type IIP SNe are understood to be RSGs with most of its hydrogen envelope intact during the SN explosion (Smartt 2009). The value of n for such a star is expected to be in the range $n = 7-12$ (Chevalier 1982). Thus the n value derived from our analysis is consistent with a RSG progenitor of SN 2004dj.

Assuming FFA as the dominant absorption process, we derive the mass-loss rate of the progenitor star of SN 2004dj as $\dot{M} = (1.37 \pm 0.11) \times 10^{-6} M_{\odot} \text{yr}^{-1}$. The progenitors of Type IIP SNe are understood to be red-supergiants whose initial masses range from 8 - 25 M_{\odot} (Heger et al. 2003). For the best studied RSGs, the range of mass-loss rates is considerably large, i.e 2×10^{-7} to $1.5 \times 10^{-5} M_{\odot} \text{yr}^{-1}$ (Jura & Kleinmann 1990; van Loon et al. 2005). The mass-loss rates of RSGs at the time of explosion is estimated using stellar evolutionary calculations as $\sim 3 \times 10^{-7}$ to $3 \times 10^{-5} M_{\odot} \text{yr}^{-1}$ (Schaller et al. 1992; Chevalier et al. 2006). The theoretical estimate of mass-loss rate for $15M_{\odot}$ models is derived as $\dot{M} = (0.84-1.6) \times 10^{-6} M_{\odot} \text{yr}^{-1}$ and for $20M_{\odot}$ models is derived as $\dot{M} = (3.0-6.2) \times 10^{-6} M_{\odot} \text{yr}^{-1}$ (Chevalier et al. 2006). Thus the mass-loss rate de-

rived for SN 2004dj from radio observations are consistent with the theoretical predictions for a progenitor star of mass $\sim 15M_{\odot}$. The progenitor mass of SN 2004dj was inferred as $15M_{\odot}$ from stellar population studies of S96 cluster (Maíz-Apellániz et al. 2004).

Mass-loss rate of the progenitor star of SN 2004dj was derived by Chakraborti et al. (2012) from X-ray emission measure as $\dot{M} = (3.2 \pm 1.1) \times 10^{-7} M_{\odot} \text{yr}^{-1}$ which is ~ 4 times lower than our mass-loss estimate. Chugai et al. (2007) derived the mass-loss rate of SN 2004dj to be $\sim 1 \times 10^{-6} M_{\odot} \text{yr}^{-1}$ for a wind velocity of 10 km s^{-1} , consistent with the mass-loss rate estimate from our analysis. Chevalier et al. (2006) derives a mass-loss rate of $\dot{M}_{-6}/w1 \sim (2-3) T_{cs5}^{3/4}$ for SN 2004dj using the first 100 days of radio data. Here \dot{M}_{-6} is the mass-loss rate in units of $10^{-6} M_{\odot} \text{yr}^{-1}$ and $w1$ is the stellar wind velocity in units of 10 km s^{-1} . T_{cs5} denotes the CSM electron temperature in units of 10^5 K. The authors compile the radio and X-ray data of all type IIP SNe available then and derive a range of mass-loss rates $(1-10) \times 10^{-6} M_{\odot} \text{yr}^{-1}$ (see Table 3) for Type IIP progenitors and our mass-loss rate estimation is consistent with this range.

6.2. Signatures of cooling

The radio light curve and spectra of Type IIP SNe can be affected by cooling. Cooling becomes important depending on various parameters of SN such as ejecta, magnetic field strength, circumstellar medium, relativistic electrons etc (Chevalier et al. 2006). The electron can lose energy by adiabatic expansion, synchrotron cooling, and IC cooling. The dominant cooling process can be identified by calculating the break frequencies and cooling time scales for different cooling processes.

One of the important signature of cooling is imprinted in the evolution of radio spectral indices. As a result of cooling the spectral index α steepens by $\Delta\alpha \sim -0.5$. This appears as a break in the spectra at a certain frequency when the electrons radiating above that characteristic frequency loses significant energy.

Assuming that the synchrotron loss time scale is equal to the age of the SN, the expression for synchrotron break frequency is given by Chevalier et al. (2006) as

$$\nu_{\text{syn}} = 240 \left(\frac{\epsilon_B}{0.1} \right)^{(-3/2)} \left(\frac{\dot{M}}{10^{-6} M_{\odot} \text{yr}^{-1}} \right)^{-3/2} \times \left(\frac{w}{10 \text{ km s}^{-1}} \right)^{3/2} \left(\frac{t}{60 \text{ days}} \right) \text{ GHz} \quad (7)$$

Assuming that the IC cooling time scale is equal to the age of the SN, the IC break frequency is (Chevalier et al. 2006)

$$\nu_{\text{IC}} = 8 \left(\frac{\epsilon_B}{0.1} \right)^{(1/2)} \left(\frac{\dot{M}}{10^{-6} M_{\odot} \text{yr}^{-1}} \right)^{1/2} \times \left(\frac{v_w}{10 \text{ km s}^{-1}} \right)^{-1/2} \left(\frac{t}{60 \text{ days}} \right) \times \left(\frac{V_s}{10^4 \text{ km s}^{-1}} \right)^4 \left(\frac{L_{\text{bol}}(t)}{10^{42} \text{ erg s}^{-1}} \right) \text{ GHz} \quad (8)$$

Chakraborti et al. (2012) derived $\epsilon_B = 0.082$ and $\epsilon_e = 0.39$ for SN 2004dj using four epochs of *Chandra* data ($\sim 42, 56, 97$ and 177 days post explosion) where the authors found prominent IC X-ray component in the first two epochs. We calculate the break frequencies corresponding to synchrotron cooling and IC cooling using the above equations at these two epochs (i.e day 42 and 56 post explosion). The value of ϵ_B is taken from (Chakraborti et al. 2012) and \dot{M} from our calculations. We use the value of shock velocity $V_s = 9.2 \times 10^3 \text{ km s}^{-1}$ (Chakraborti et al. 2012). The bolometric luminosity during the plateau is $L_{\text{bol}} \sim 0.89 \times 10^{42} \text{ ergs}$ (Zhang et al. 2006). Assuming a wind velocity of 10 km s^{-1} , and temperature of 10^4 K , the ν_{syn} and ν_{IC} corresponding to day 42 and 56 days post explosion are $\sim 141, 4 \text{ GHz}$ and $188, 5 \text{ GHz}$ respectively. The synchrotron break frequency is too high to observe with the VLA during our observation epochs. The IC cooling break frequency is within our observation frequencies and with the multi-frequency observations of SN 2004dj, we can look for this signature in the data. In Figure 2, We plot the evolution of spectral indices between successive frequencies, 1.06/1.39, 1.39/4.99, 4.99/8.46 GHz with time for SN 2004dj. The spectral index values of 4.86/8.46 GHz approaches values ~ -1 and lower during an extended period starting from \sim day 50 (see Figure 2). Thus we see the IC cooling break at $\sim 5 \text{ GHz}$, roughly consistent with the above calculation. The optical bolometric light curve is in the plateau phase during the same period (Zhang et al. 2006). The dense optical photon medium in the plateau phase of the SN provides seed photons and enhances the IC cooling. This kind of a dip in the spectral index is seen for the second time in a type IIP supernova after SN 2012aw (Yadav et al. 2014).

We establish IC cooling as the dominant cooling process as there is evidence of cooling break at $\sim 5 \text{ GHz}$ in the radio spectral evolution. Here, we calculate the cooling timescale at $\sim 5 \text{ GHz}$ for IC and synchrotron cooling process to further investigate this.

The ratio of synchrotron cooling time scale to the adiabatic expansion timescale is (Chevalier et al. 2006)

$$\frac{t_{\text{syn}}}{t} \approx 2.0 \left(\frac{\epsilon_B}{0.1} \right)^{-3/4} \left(\frac{\dot{M}_{-6}}{v_{w1}} \right)^{-3/4} \left(\frac{\nu}{10 \text{ GHz}} \right)^{-1/2} \times \left(\frac{t}{10 \text{ days}} \right)^{1/2} \quad (9)$$

The ratio of Compton cooling timescale to the adiabatic expansion timescale is

$$\frac{t_{\text{Comp}}}{t} \approx 0.18 \left(\frac{L_{\text{bol}}}{2 \times 10^{42} \text{ erg s}^{-1}} \right)^{-1} \left(\frac{\epsilon_B}{0.1} \right)^{1/4} \left(\frac{\dot{M}_{-6}}{v_{w1}} \right)^{1/4} \times V_{s4}^2 \left(\frac{\nu}{10 \text{ GHz}} \right)^{-1/2} \left(\frac{t}{10 \text{ days}} \right)^{1/2} \quad (10)$$

In general, lower values of ϵ_B and \dot{M} favours IC cooling and especially at early times. We estimate the ratios t_{Comp}/t and t_{syn}/t at ~ 42 and 56 days post explosion using the above equations as $\sim 0.9, 5.3$ and $1.1, 6.1$ respectively. While the ratios of cooling time-scale is close to 1 for IC cooling, the ratios are much higher for synchrotron cooling; clearly indicates that synchrotron cooling is not plausible. Thus these numbers favour the IC cooling to be in operation during these epochs at the SN shock. This is in agreement with the detection of non-thermal IC component in the X-ray spectra of SN 2004dj during the first two epochs of observations (\sim day 42 and 56 post explosion) by Chakraborti et al. (2012). Thus both cooling time scale and break frequency calculations supports the IC cooling happening at the SN shock during the plateau phase.

Chevalier et al. (2006) predicts a flattened light curve and a dip in the radio light curve of Type IIP SNe especially at higher frequencies as a signature of IC cooling. However, from our error bars on flux densities and cadence of observation, it is difficult to look for a flattening or small dip in the light curve as predicted by Chevalier et al. (2006). Cooling processes and its effect on the radio light curves could be modelled better with a good quality and high cadence early time data at radio frequencies.

6.3. Circumstellar Electron Temperature

The circumstellar electron temperature is an uncertain parameter since the effect of SN radiation on the circumstellar gas needs to be estimated from the CSM models (Chevalier & Fransson 2003; Chevalier et al. 2006). Calculations on Type IIL SNe suggest that the temperature at unit optical depth $T_{\text{cs}} \sim 3 \times 10^4 \text{ K}$ for $\dot{M}_{-6}/w1 = 3$ and $T_{\text{cs}} \sim 1 \times 10^5 \text{ K}$ for $\dot{M}_{-6}/w1 = 10$ (Lundqvist & Fransson 1988). The mass-loss rate

Table 3. Comparison of SN 2004dj parameters with other radio/X-ray bright Type IIP SNe.

SN	Parent Galaxy	Distance (Mpc)	L_{radio} (erg s ⁻¹ Hz ⁻¹)	L_{Xray} (erg s ⁻¹)	\dot{M} (10 ⁻⁶ M_{\odot} yr ⁻¹)	Progenitor mass (M_{\odot})	References
SN 1999em	NGC 1637	11.7 ± 1.0	2.2 × 10 ²⁵	9 × 10 ³⁷	0.9 ^a	<15	1,2,3,4
SN 1999gi	NGC 3184	11.1 ^{+2.0} _{-1.8}	— [*]	1.6 × 10 ³⁷	~ 1 ^b	<12	1,2,3,5
SN 2002hh	NGC 6946	5.5 ± 1.0	1.3 × 10 ²⁵	4 × 10 ³⁸	1.2 ^a	—	3,6,7,8
SN 2004dj	NGC 2403	3.47	2.5 × 10²⁵	1.5 × 10³⁸	1.4^c, (0.2 - 0.5)^a, 0.3^b	15, ~ 12, >20	3,9,10,11
SN 2004et	NGC 6946	5.5 ± 1.0	8.7 × 10 ²⁵	(2.1 - 3) × 10 ³⁸	(1.6-1.8) ^a , ~ 2 ^b	15 ⁺⁵ ₋₂	3,6,12,13
SN 2011ja	NGC 4945	3.36 ± 0.09	7.3 × 10 ²⁴	(1.3 - 5.5) × 10 ³⁸	0.12 - 1.9 ^b	—	14,15
SN 2013ej	M74	9.6 ± 0.7	— [*]	~ (1 - 4) × 10 ⁴²	2.6 ^b	—	16,17
SN 2012aw	M95	10	7.2 × 10 ²⁵	9.2 × 10 ³⁸	~ 3.2-10 ^b	14-26, 17-18	18,19,20,21,22
SN 2017eaw	NGC 6946	5.86 ± 0.76	1.7 × 10 ²⁵	1.1 × 10 ³⁹	—	—	22,23,24

NOTE—This table is adapted from a similar table published by Chevalier et al. (2006) with more SNe added.

NOTE—References: (1) Leonard et al. (2002), (2) Smartt et al. (2003), (3) Chevalier et al. (2006), (4) Pooley et al. (2002), (5) Schlegel (2001), (6) Li et al. (2005), (7) Pooley & Lewin (2002), (8) Beswick et al. (2005), (9) Chakraborti et al. (2012), (10) Maíz-Apellániz et al. (2004), (11) Vinkó et al. (2006), (12) Misra et al. (2007), Li et al. (2005), (13) Argo et al. (2005), (14) Chakraborti et al. (2013), (15) Mouhcine et al. (2005), (16) Chakraborti et al. (2016) (17) Bose et al. (2015), (18) Kochanek et al. (2012), (19) Immler & Brown (2012), (20) Fraser et al. (2012), (21) Van Dyk et al. (2012), (22) Argo et al. (2017), (23) Bose & Kumar (2014), (24) Grefenstette et al. (2017).

NOTE—X-ray luminosity in the energy range of 0.5 - 8 KeV for all SNe except SN 2011ja, SN 2017eaw (0.3 - 10 KeV) and SN 2012aw (0.2 - 10 KeV). Radio luminosity is spectral luminosity at ~ 5 GHz. Where possible, the X-ray and radio luminosities are taken at the peak of the light curve and for others, the limits of peak flux density is used. The mass of the progenitor stars are from the pre-explosion observations of the SN site. The listed mass-loss rates are from X-ray/radio observations and modelling.

^aThe mass-loss rate is estimated from radio analysis and modelling assuming a stellar wind velocity of 10 km s⁻¹. While for SN 1999em, SN 2002hh, SN 2004et Chevalier et al. (2006) and for SN 2012aw Yadav et al. (2014) calculate mass-loss rates assuming a CSM electron temperature of 10⁵ K, we recalculate these numbers for an electron temperature of 10⁴ K for comparison since we used electron temperature of 10⁴ K to calculate the mass-loss rate of SN 2004dj.

^{*}Not detected in radio.

^bThe mass-loss rates are estimated from the X-ray observations assuming a stellar wind velocity of 10 km s⁻¹.

^cThe mass-loss rate estimated for SN 2004dj from this work assuming a stellar wind velocity of 10 km s⁻¹ and CSM electron temperature of 10⁴ K.

depends on T_e as $\dot{M} \propto T_e^{0.68}$ (Weiler et al. 1986), and hence the uncertainty in T_e will cause significant errors in \dot{M} . Assuming an electron temperature of $T_e = 10^4$ K, we derive the mass-loss rate of SN 2004dj progenitor as $\dot{M} = (1.37 \pm 0.11) \times 10^{-6} M_{\odot} \text{yr}^{-1}$ from our radio analysis and modelling. However, if we assume electron temperature $T_e = 10^5$ K, the mass-loss rate will be $\dot{M} = (6.56 \pm 0.66) \times 10^{-6} M_{\odot} \text{yr}^{-1}$. This is ~ 20 times larger than the mass-loss rate derived from X-ray observations, i.e. $(3.2 \pm 1.1) \times 10^{-7} M_{\odot} \text{yr}^{-1}$ (Chakraborti et al. 2012). It is also important to note that lower values of \dot{M} favours IC cooling (Chevalier et al. 2006; Chakraborti et al. 2012). If we

use $\dot{M} = (6.56 \pm 0.66) \times 10^{-6} M_{\odot} \text{yr}^{-1}$, the ratio of cooling timescales are $t_{\text{Comp}}/t = 1.7$ and $t_{\text{syn}}/t = 1.9$ on day 56 post explosion. Since both the ratios are much above 1, these numbers do not favour IC cooling. But there are several lines of evidences including the prominent IC X-ray component on day 56 post explosion (Chakraborti et al. 2012) showing that IC cooling is happening at the SN shock during this time as discussed in §6.2. Thus the mass-loss rate derived for SN 2004dj assuming a electron temperature of $T_e = 10^5$ K is too high to explain the observational signature of IC cooling. We suggest the electron temperature of the CSM to be ~10⁴ K rather than 10⁵ K for SN 2004dj. We also note

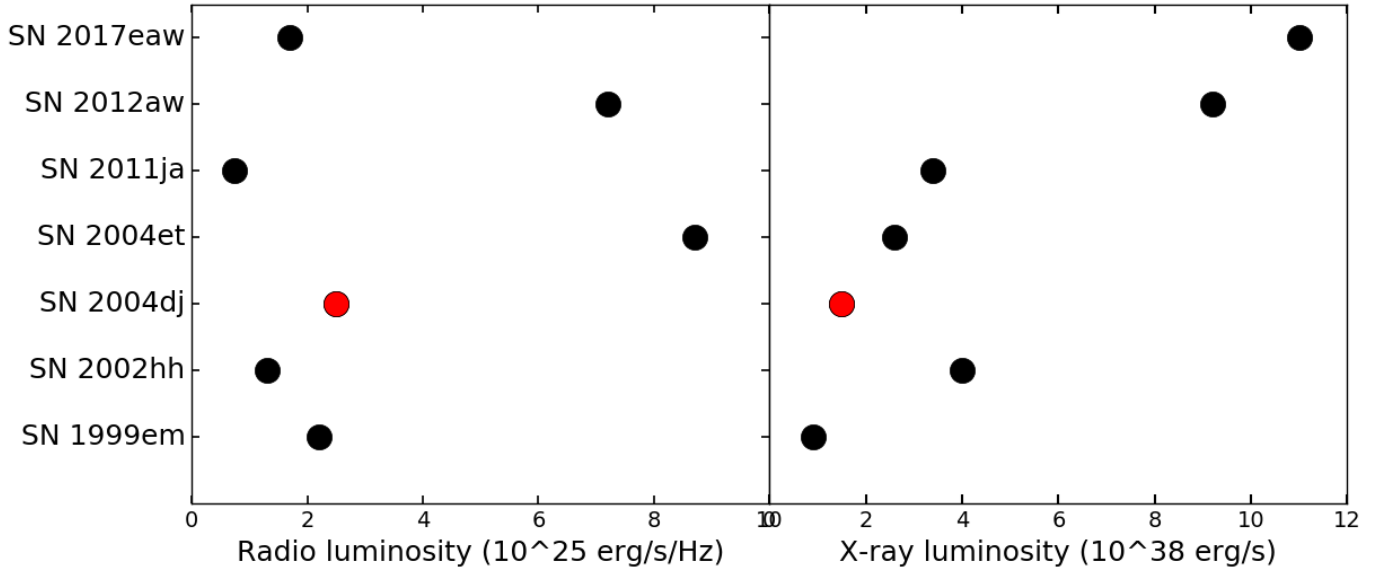


Figure 5. Left panel: Radio spectral luminosity at ~ 5 GHz of Type IIP SNe Right panel: X-ray luminosity in the energy range of 0.5 - 8 KeV for all SNe except SN 2017eaw (0.3 - 10 KeV) and SN 2012aw (0.2 - 10 KeV). Where possible, the X-ray and radio luminosities are taken at the peak of the light curve and for others, the limits of peak flux density is used. We include only the Type IIP SNe with both X-ray and radio detection.

that Misra et al. (2007) deduce the CSM temperature of another Type IIP SN 2004et as 10^4 K from combined X-ray and radio data which has marginally higher wind density (see Table 3) and mass-loss rates (Misra et al. 2007) as that of SN 2004dj.

6.4. Comparison of SN 2004dj with other Type IIP SNe

Even though Type IIP is the most commonly observed variety of core-collapse SNe in the optical band, only few of them are known radio/X-ray emitters. SN 2004dj being one of the best observed Type IIP SNe in the radio bands, here we compare the properties of SN 2004dj with other radio/X-ray bright Type IIP SNe; SN 1999em, SN 1999gi, SN 2002hh, SN 2004et, SN 2011ja, SN 2013ej, SN 2012aw and SN 2017eaw. The physical parameters of these SNe along with the references are compiled in Table 3. We also plot the radio and X-ray luminosities of Type IIP SNe that was detected in both radio and X-ray bands in Figure 5.

The radio and X-ray luminosities of SN 2004dj is comparable to that of SN 1999em and SN 2002hh (see Fig 5) and is suggestive of comparable CSM densities. The mass-loss rate of the progenitor of SN 1999em and SN 2002hh are $\sim 0.9 \times 10^{-6} M_{\odot}\text{yr}^{-1}$ and $\sim 1.2 \times 10^{-6} M_{\odot}\text{yr}^{-1}$ respectively (Chevalier et al. 2006) for a CSM temperature of $T_e = 10^4$ K. This is similar to the mass-loss rate derived for SN 2004dj from our radio analysis (see Table 3). While the X-ray luminosity of SN 2004et is comparable to that of SN 2004dj, the radio luminosity of SN 2004et is larger than (~ 3.5 times) SN 2004dj and could be indicative of slightly larger wind densities. The

mass-loss rate of SN 2004et is derived from X-ray observations to be $\dot{M} \sim 2 \times 10^{-6} M_{\odot}\text{yr}^{-1}$ (Misra et al. 2007) and $\dot{M} \sim (1.6 - 1.8) \times 10^{-6} M_{\odot}\text{yr}^{-1}$ (Chevalier et al. 2006). These numbers are marginally larger than the mass-loss rate of SN 2004dj derived from our analysis.

SN 2012aw has a larger X-ray luminosity (~ 6 times) and radio luminosity (~ 3 times; Yadav et al. 2014) as compared to SN 2004dj (see Fig 5). The mass-loss rate is $\dot{M} \sim 3.2 \times 10^{-6} M_{\odot}\text{yr}^{-1}$ from X-ray analysis (Kochanek et al. 2012) which is larger than the mass-loss rate of SN 2004dj.

It is found that \dot{M} depends on the metallicity of the regions of SNe as $\dot{M} \propto Z^{0.5}$ (Schaller et al. 1992; Heger et al. 2003). The metallicity of the regions of occurrence of SN 1999em (Smartt et al. 2003), SN 2004et (Li et al. 2005) and SN 2004dj (Wang et al. 2005) are (1-2), (0.3-1) and $\sim 0.4 Z_{\odot}$ respectively. This will have a minor effect in the \dot{M} comparison discussed above.

To summarize, the estimate of mass-loss rate of the progenitor star depends on various physical parameters including CSM electron temperature and metallicity of the site of SN explosion. A fair comparison is not possible unless these quantities are well constrained by either observations or modelling. However, the mass-loss rates of Type IIP SNe progenitors deduced from radio and X-ray observations and modelling span over a range of $\sim (0.1 - 10) \times 10^{-6} M_{\odot}\text{yr}^{-1}$.

7. SUMMARY

We carried out detailed radio observations of Type IIP supernova SN 2004dj at frequencies ranging from 0.24 -

43 GHz at ages from 1.12 days to ~ 12 years post discovery. We model the radio observations with standard mini-shell model (Chevalier 1982). Both FFA and SSA models fit with the data reasonably well and it is difficult to conclude either of them as the dominant absorption process from the modelled parameters. However, from the optical line velocity measurements, we infer FFA as the dominant absorption process which is consistent with the prediction by Chevalier et al. (2006). The radio observations and modelling are consistent with the interaction of the SN with an outer ejecta density profile $\rho \sim r^{-11.4}$ with a circumstellar density field created by a pre-SN steady stellar wind. We derive the shock deceleration parameter $m \sim 0.9$ ($R \sim t^m$) indicative of a mildly decelerating blast wave. Assuming FFA to be the dominant absorption process, we derive the mass-loss rate of the progenitor star as $\dot{M} = (1.37 \pm 0.11) \times 10^{-6} M_{\odot} \text{yr}^{-1}$. The mass-loss rate derived from our observations are consistent with the theoretical predictions for a progenitor star of mass $M \sim 15 M_{\odot}$. The mass-loss rate derived from our analysis is ~ 3 times larger than the value derived by Chevalier et al. (2006) for SN 2004dj from early radio data. However, our mass-loss estimate is consistent with the range of RSG mass-loss rates of type IIP SNe (Chevalier et al. 2006). Chakraborti et al. (2012) estimated the mass-loss rate, $\dot{M} = 3.2 \times 10^{-7} M_{\odot} \text{yr}^{-1}$ from X-ray emission measure and is ~ 4 times smaller than the value derived from our analysis. We also present the evolution of radio spectral indices with 1.06, 1.4, 4.86, 8.46 GHz flux density measurements. The spectral indices steepen to values of -1 around day 50 and continues till \sim day 125, especially at higher frequencies (4.86/8.46), suggestive of electron cooling. During this period, the optical light curve is in the

plateau phase. We estimate the cooling time scale for both IC and synchrotron cooling and interpret the steepening as a signature of IC cooling at the SN shock.

SN 2004dj is the only Type IIP SN with radio data covering two order of magnitudes in time and frequency and this allowed us to study this SN as a prototype of Type IIP SNe. We compare the properties of SN 2004dj with other radio/X-ray bright Type IIP SNe and find that SN 2004dj is a normal type IIP SNe with very similar CSM properties as that of SN 1999em and SN 2002hh.

We thank the anonymous referee for the constructive comments. We thank Kurt Weiler for providing us the early VLA data for this supernova. We acknowledge Roger Chevalier for his comments on the manuscript. P.C. acknowledges support from the Department of Science and Technology via SwaranaJayanti Fellowship award (file no.DST/SJF/PSA-01/2014-15). A.R. acknowledges Raja Ramana Fellowship of DAE, Govt of India. We thank the staff of the GMRT that made these observations possible. GMRT is run by the National Centre for Radio Astrophysics of the Tata Institute of Fundamental Research. The National Radio Astronomy Observatory is a facility of the National Science Foundation operated under cooperative agreement by Associated Universities, Inc.

Software: AIPS (van Moorsel et al. 1996)

Facilities: Giant Metrewave Radio Telescope, Karl J. Jansky Very Large Array

REFERENCES

- Argo, M. K., Muxlow, T. W. B., Beswick, R. J., Pedlar, A., & Marcaide, J. M. 2004, IAUC, 8399, 3
- Argo, M. K., Beswick, R. J., Muxlow, T. W. B., et al. 2005, Mem. Soc. Astron. Italiana, 76, 565
- Argo, M., Torres, M. P., Beswick, R., & Wrigley, N. 2017, The Astronomer's Telegram, 10472,
- Beswick, R. J., Muxlow, T. W. B., Argo, M. K., et al. 2005, ApJL, 623, L21
- Beswick, R. J., Fenech, D., Thrall, H., et al. 2005, IAUC, 8572, 1
- Bose, S., & Kumar, B. 2014, ApJ, 782, 98
- Bose, S., Sutaria, F., Kumar, B., et al. 2015, ApJ, 806, 160
- Chakraborti, S., Ray, A., Smith, R., et al. 2013, ApJ, 774, 30
- Chakraborti, S., Ray, A., Smith, R., et al. 2016, ApJ, 817, 22
- Chakraborti, S., Yadav, N., Ray, A., et al. 2012, ApJ, 761, 100
- Chandra, P., & Ray, A. 2004, IAUC, 8397, 3
- Chevalier, R. A. 1982, ApJ, 259, 302
- Chevalier, R. A. 1984, ApJL, 285, L63
- Chevalier, R. A. 1996, Radio Emission from the Stars and the Sun, 93, 125
- Chevalier, R. A. 1998, ApJ, 499, 810
- Chevalier, R. A., & Fransson, C. 2003, Supernovae and Gamma-Ray Bursters, 598, 171
- Chevalier, R. A., & Fransson, C. 2006, ApJ, 651, 381
- Chevalier, R. A., Fransson, C., & Nymark, T. K. 2006, ApJ, 641, 1029

- Chugai, N. N., Fabrika, S. N., Sholukhova, O. N., et al. 2005, *Astronomy Letters*, 31, 792
- Chugai, N. N., Chevalier, R. A., & Utrobin, V. P. 2007, *ApJ*, 662, 1136
- de Jager, C., Nieuwenhuijzen, H., & van der Hucht, K. A. 1988, *A&AS*, 72, 259
- Falk, S. W., & Arnett, W. D. 1977, *ApJS*, 33, 515
- Filippenko, A. V. 1997, *ARA&A*, 35, 309
- Fraser, M., Maund, J. R., Smartt, S. J., et al. 2012, *ApJL*, 759, L13
- Fransson, C., & Björnsson, C.-I. 1998, *ApJ*, 509, 861
- Freedman, W. L., Madore, B. F., Gibson, B. K., et al. 2001, *ApJ*, 553, 47
- Grasberg, E. K., Imshenik, V. S., & Nadyozhin, D. K. 1971, *Ap&SS*, 28, 3
- Grefenstette, B., Harrison, F., & Brightman, M. 2017, *The Astronomer's Telegram*, 10427,
- Heger, A., Fryer, C. L., Woosley, S. E., Langer, N., & Hartmann, D. H. 2003, *ApJ*, 591, 288
- Immler, S., & Brown, P. J. 2012, *The Astronomer's Telegram*, 3995,
- Jura, M., & Kleinmann, S. G. 1990, *ApJS*, 73, 769
- Kochanek, C. S., Khan, R., & Dai, X. 2012, *ApJ*, 759, 20
- Kotak, R., Meikle, P., van Dyk, S. D., Höflich, P. A., & Mattila, S. 2005, *ApJL*, 628, L123
- Korcakova, D., Mikulasek, Z., Kawka, A., et al. 2005, *Information Bulletin on Variable Stars*, 5605, 1
- Leonard, D. C., Filippenko, A. V., Li, W., et al. 2002, *AJ*, 124, 2490
- Li, W., Van Dyk, S. D., Filippenko, A. V., & Cuillandre, J.-C. 2005, *PASP*, 117, 121
- Li, W., Van Dyk, S. D., Filippenko, A. V., et al. 2006, *ApJ*, 641, 1060
- Lundqvist, P., & Fransson, C. 1988, *A&A*, 192, 221
- Maíz-Apellániz, J., Bond, H. E., Siegel, M. H., et al. 2004, *ApJL*, 615, L113
- Maiz-Apellaniz, J. 2004, *IAUC*, 8385, 2
- Matzner, C. D., & McKee, C. F. 1999, *ApJ*, 510, 379
- Maund, J. R., & Smartt, S. J. 2005, *MNRAS*, 360, 288
- Maund, J. R., Smartt, S. J., & Danziger, I. J. 2005, *MNRAS*, 364, L33
- Misra, K., Pooley, D., Chandra, P., et al. 2007, *MNRAS*, 381, 280
- Mouhcine, M., Ferguson, H. C., Rich, R. M., Brown, T. M., & Smith, T. E. 2005, *ApJ*, 633, 810
- Nadyozhin, D. K. 2003, *MNRAS*, 346, 97
- Nakano, S., Itagaki, K., Bouma, R. J., Lehky, M., & Hornoch, K. 2004, *IAUC*, 8377, 1
- Nayana, A. J., & Chandra, P. 2017, *The Astronomer's Telegram*, 10534,
- Nieuwenhuijzen, H., & de Jager, C. 1990, *A&A*, 231, 134
- Patat, F., Benetti, S., Pastorello, A., Filippenko, A. V., & Aceituno, J. 2004, *IAUC*, 8378, 1
- Pooley, D., & Lewin, W. H. G. 2002, *IAUC*, 8024, 2
- Pooley, D., Lewin, W. H. G., Fox, D. W., et al. 2002, *ApJ*, 572, 932
- Pooley, D., & Lewin, W. H. G. 2004, *IAUC*, 8390, 1
- Pilyugin, L. S., Vílchez, J. M., & Contini, T. 2004, *A&A*, 425, 849
- Reimers, D. 1977, *A&A*, 61, 217
- Schaller, G., Schaerer, D., Meynet, G., & Maeder, A. 1992, *A&AS*, 96, 269
- Schlegel, E. M. 2001, *ApJL*, 556, L25
- Smartt, S. J., Maund, J. R., Gilmore, G. F., et al. 2003, *MNRAS*, 343, 735
- Smartt, S. J., Maund, J. R., Hendry, M. A., et al. 2004, *Science*, 303, 499
- Smartt, S. J., Eldridge, J. J., Crockett, R. M., & Maund, J. R. 2009, *MNRAS*, 395, 1409
- Smartt, S. J. 2009, *ARA&A*, 47, 63
- Smartt, S. J., Maund, J. R., Hendry, M. A., et al. 2004, *Science*, 303, 499
- Smith, N., Li, W., Filippenko, A. V., & Chornock, R. 2011, *MNRAS*, 412, 1522
- Stockdale, C. J., Sramek, R. A., Weiler, K. W., et al. 2004, *IAUC*, 8379, 1
- Sugerman, B., Seeds Collaboration, Sings Legacy, P., & van Dyk, S. 2005, *IAUC*, 8489, 2
- Van Dyk, S. D., Weiler, K. W., Sramek, R. A., Rupen, M. P., & Panagia, N. 1994, *ApJ*, 432, L115
- Van Dyk, S. D., Li, W., & Filippenko, A. V. 2003, *PASP*, 115, 1289
- Van Dyk, S. D., Cenko, S. B., Poznanski, D., et al. 2012, *ApJ*, 756, 131
- van Moorsel, G., Kemball, A., & Greisen, E. 1996, *Astronomical Data Analysis Software and Systems V*, 101, 37
- van Loon, J. T., Cioni, M.-R. L., Zijlstra, A. A., & Loup, C. 2005, *A&A*, 438, 273
- Vinkó, J., Takáts, K., Sárneczky, K., et al. 2006, *MNRAS*, 369, 1780
- Wang, X., Yang, Y., Zhang, T., et al. 2005, *ApJL*, 626, L89
- Weiler, K. W., Sramek, R. A., Panagia, N., van der Hulst, J. M., & Salvati, M. 1986, *ApJ*, 301, 790
- Weiler, K. W., Panagia, N., Montes, M. J., & Sramek, R. A. 2002, *ARA&A*, 40, 387
- Yadav, N., Ray, A., Chakraborti, S., et al. 2014, *ApJ*, 782, 30
- Zhang, T., Wang, X., Li, W., et al. 2006, *AJ*, 131, 2245